

Particle-size effect on the compressibility of nanocrystalline aluminaB. Chen,¹ D. Penwell,¹ L. R. Benedetti,² R. Jeanloz,³ and M. B. Kruger¹¹*Department of Physics, University of Missouri, Kansas City, Missouri 64110*²*Department of Physics, University of California, Berkeley, California 94720*³*Departments of Earth and Planetary Science and of Astronomy, University of California, Berkeley, California 94720*

(Received 15 January 2002; published 4 October 2002)

Room-temperature x-ray diffraction to 60 GPa yields zero-pressure bulk modulus values of $K_{67}=238 \pm 3$ GPa and $K_{37}=172 \pm 3$ GPa for nanocrystalline γ -alumina (Al_2O_3) with particle sizes of 67 and 37 nm, respectively. Combined with the results of previous high-pressure x-ray studies of 20 and 6 nm nanocrystalline Al_2O_3 , it is found that compressibility increases with decreasing particle size. A new phase was detected at pressures above 51 and 56 GPa for γ - Al_2O_3 of 67 and 37 nm, respectively.

DOI: 10.1103/PhysRevB.66.144101

PACS number(s): 62.50.+p, 61.10.Nz, 61.50.Ks, 64.70.Kb

INTRODUCTION

The study of nanocrystalline materials with dimensions less than ~ 100 nm is an active area of research in physics, chemistry, and engineering.^{1,2} Nanocrystals have large surface-to-volume ratios, and surface effects take on a significance that is normally inconsequential for bulk materials. The small volume can confine free carriers, allowing observation of quantum behavior. While of immense intrinsic interest, the study of nanocrystals is also propelled by technological promise. Various physical properties such as hardness, melting temperature, sintering ability, and electronic structure may be dependent upon particle size.³⁻⁵ Additionally, the barrier height between two phases of a material has been found to depend on the size of the nanocrystal.⁶ That nanomaterials may display novel or enhanced properties compared to traditional materials opens up possibilities for new technological applications.

There have been numerous studies on the relationship between the size of nanocrystals and their properties. It has been reported that the melting temperature decreases with decreasing particle size,⁵ for example, but the effect of particle size on the stability of crystalline phases appears to be more varied.⁶⁻¹¹ Some nanocrystals show elevated phase transition pressures with decreasing particle size^{7,9,12} while others exhibit reduced phase transition pressures with decreasing particle size.^{13,14} Whereas the elevation of nanocrystal transition pressures is explained in terms of surface-energy differences between the phases involved, it is suggested that a larger volume change, for the nanocrystal, upon the transition can reduce the phase-transition pressure. To increase the amount of experimental information available on structural stability as well as to explore the relationship between the size of a particle and its equation of state, nanocrystalline alumina has been studied.

Alumina is one of the most important ceramics, having applications ranging from electronics to lasers. Although α -alumina is the thermodynamically stable phase of bulk Al_2O_3 under a wide range of pressures and temperatures, recent theoretical and experimental work has determined that under high pressure and temperature, α - Al_2O_3 converts to the Rh_2O_3 (II) structure.¹⁵⁻¹⁷ The structural change is of sig-

nificance in broadening our understanding of the properties of Al_2O_3 .

Molecular dynamic simulations indicate that the γ -phase of alumina, which crystallizes in the defect spinel structure, may be the thermodynamically stable phase of Al_2O_3 for specific surface areas greater than ~ 175 m²/g, the γ phase being stabilized compared to the α phase because it has a lower surface free energy.^{18,19} Spherical alumina particles of such high specific surface area would have diameters less than 10 nm. Recent heat-capacity measurements on nanocrystalline α and γ alumina suggest that the higher energy for the α phase may be due to a few high-energy surface sites.^{19,20}

γ - Al_2O_3 is widely used in technology as a catalyst, catalyst carrier, absorbent, coating, and soft abrasive because of its fine particle size and catalytic activity. Many approaches of synthesis, such as microwave sintering, plasma-assisted sintering, and high-pressure sintering, have been explored in order to produce highly dense γ - Al_2O_3 without excessive grain growth.²¹⁻²³ High-pressure sintering provides an attractive opportunity to obtain fully dense nanocrystalline alumina.²⁴

The high-pressure compaction of nanophase γ -alumina has recently been studied up to pressures of 4.5 GPa and temperatures of up to 870 °C in order to better understand the sintering process.²⁵ Using x-ray diffraction, 20 nm particles of γ alumina have been studied up to 3.8 GPa, and 6 nm particles have been studied up to 30 GPa.^{26,27} No new phases were observed and equations of state were obtained for both sizes of particles. In the present article, we report on x-ray diffraction experiments performed up to a pressure of 60 GPa to measure the compressibility of nanocrystalline γ - Al_2O_3 as a function of particle size.

EXPERIMENT

In separate experiments, nanocrystalline γ alumina, with average particle sizes of 67 and 37 nm (Nanophase Technologies Corporation, IL) was compressed quasistatically to pressures up to ~ 60 GPa, in a Mao-Bell type diamond anvil cell, at room temperature.²⁸ A spring-steel gasket, with a chamber having a diameter of 120 μm , was used to contain the sample between diamonds having 350

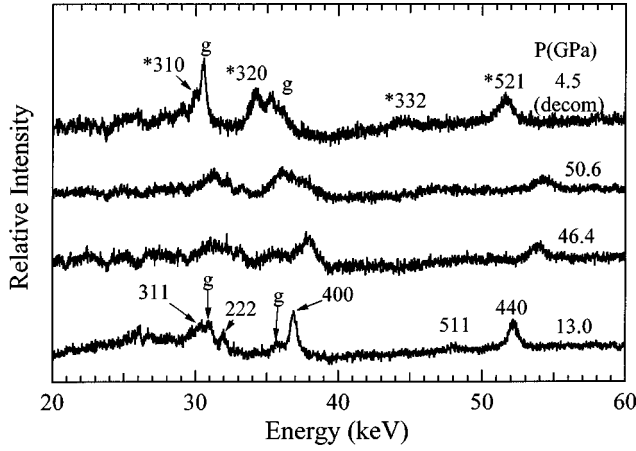


FIG. 1. Representative x-ray diffraction patterns from quasi-hydrostatically compressed samples of γ - Al_2O_3 with an average size of 67 nm. The Miller indices are labeled for each reflection, with those from the high-pressure phase having an asterisk. The peaks labeled with a “g” are due to diffraction from gold. The patterns shown were collected at NSLS with $2\theta = 9.958 \pm 0.002^\circ$.

μm culets. A 4:1 mixture of methanol:ethanol was used as a pressure-transmitting medium in order to maintain a quasi-hydrostatic environment. In addition, a small amount of gold powder (<2%) was included to determine the pressure, using the equation of state of gold.²⁹ Energy-dispersive x-ray diffraction was performed at beamline X17C of the National Synchrotron Light Source (NSLS), with a 2θ of $9.958 \pm 0.002^\circ$ and $10.011 \pm 0.002^\circ$ for experiments on 67 and 37 nm γ alumina, respectively. The x-ray beam produced by the superconducting wiggler at NSLS was typically apertured to $\sim 20 \times 20 \mu\text{m}$. X-ray diffraction patterns were collected at pressure intervals of several GPa. Due to the low x-ray scattering power of alumina, the diffraction patterns have a relatively low signal-to-noise ratio even with data collection times of 1–2 h per pattern.

RESULTS AND DISCUSSION

The evolution of diffraction patterns with pressure is shown in Fig. 1 for the 67 nm particles. The patterns from 37 nm particles are similar, and the 311, 222, 400, and 440 x-ray diffraction lines were obtained from both sized nanocrystals of γ alumina. The pressure dependence of the d spacings and the unit cell volume from 0 to ~ 50 GPa is summarized in Figs. 2–4. We determined the lattice parameter of γ alumina at each pressure, using a weighted average of the d spacings, and analyzed the data in terms of the Birch-Murnaghan (Eulerian finite strain) equation of state³⁰

$$F_V = K[1 - 1.5(4 - K')f_V]. \quad (1)$$

Here, the negative of the Eulerian strain measure f_V and normalized pressure F_V are defined as

$$f_V = 0.5 \left[\left(\frac{V}{V_0} \right)^{-2/3} - 1 \right] \quad (2)$$

$$F_V = P[3f_V(1 + 2f_V)^{2.5}]^{-1}, \quad (3)$$

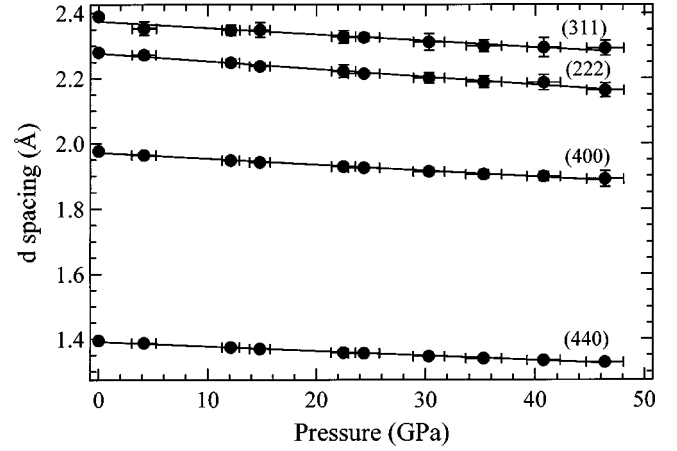


FIG. 2. Pressure dependence of the d spacings of 67 nm γ alumina. All of the data were collected upon compression, and the solid lines are guides for the eye.

with the unit-cell volume at zero pressure V_0 measured as $493 \pm 2.6 \text{ \AA}^3$. There is no discernable difference in the zero-pressure volumes of 67 and 37 nm γ alumina.

The intercept and slope of the data cast as F - f yield the bulk modulus K and its pressure derivative K' at zero pressure, respectively. Fits to the data yield $K = 238 \pm 3$ GPa and $K' = 172 \pm 3$ GPa for quasi-hydrostatically compressed γ alumina of 67 and 37 nm, respectively, with K' constrained to be 4 for both cases. For 67 nm particles, fits for K and K' yield 248 ± 6 GPa and 3.2 ± 0.5 , respectively, while K and K' for the 37 nm crystallites are 151 ± 9 GPa and 5.7 ± 0.6 , respectively. For comparison, the bulk modulus of α alumina is 254 GPa, close to the bulk modulus of the 67 nm particles of γ alumina.³¹ This is remarkable because the unit-cell volume of γ alumina is 30% greater than that of α alumina.

The bulk moduli of the 67 and 37 nm particles can be compared with previously reported data on 20 and 6 nm γ -alumina particles.^{26,27} The volume-pressure data, measured between 0–3.8 GPa for 20 nm particles were fit using both the Birch and first-order Bridgman equations.²³ The Birch

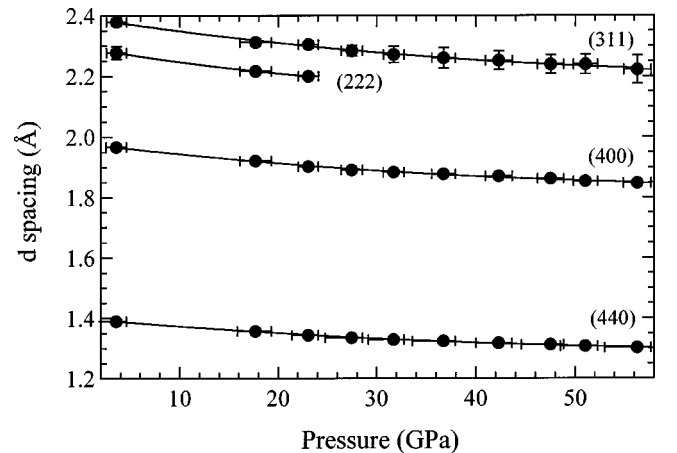


FIG. 3. Pressure dependence of the d spacings of 37 nm γ alumina. All of the data were collected upon compression, and the solid lines are guides for the eye.

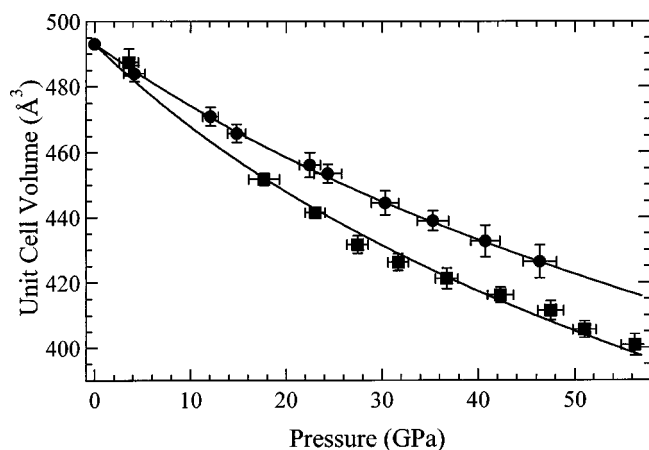


FIG. 4. Quasihydrostatic equation of state of nanocrystalline γ alumina. The circles represent data from 67 nm particles and the squares represent data from 37 nm particles, with the solid curves being Birch-Murnaghan fits to the data.

equation of state is identical to the Birch-Murnaghan equation of state, with K' constrained to be 4, allowing for a direct comparison of the 20 nm results with our 67 and 37 nm particle data. Therefore the result from the fit to the Birch equation of state $K_{20}=153\pm 13$ GPa, is what is used for comparison. Volume-pressure data from 6 nm particles for pressures up to 16 GPa were fit to the Birch-Murnaghan equation of state and yielded $K_6=152\pm 8$ GPa and $K'=6.8\pm 0.8$.²⁷ Combining the data from the two previous studies with the present work shows that compressibility increases systematically with decreasing particle size from 67 to 20 nm, and is approximately constant between 20 and 6 nm (Fig. 5). For a correct comparison between all of the data, the value for the bulk modulus of the 6 nm crystallites should be obtained by constraining $K'=4$, (or alternatively, allowing K' to float for all of the other data), but this result is not available. However, since K' is greater than 4, the quoted value of $K_6=152$ GPa is greater than the value of K that would be obtained by a fit with K' constrained to be 4. Thus,

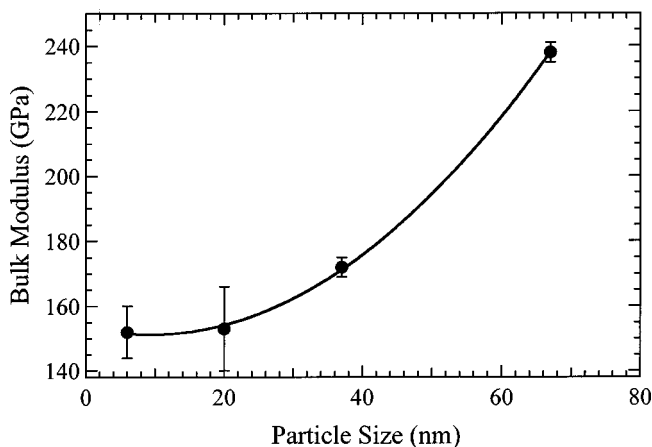


FIG. 5. Size dependence of the bulk modulus of nanocrystalline γ alumina, combining our results for 37 and 67 nm with those of Refs. 26 and 27 for 20 and 6 nm. The curve serves as a guide for the eye.

rather than flattening out, as indicated in Fig. 5, the particle size dependence of the bulk modulus may continue to decrease, with decreasing particle size, between 20 and 6 nm. The lattice parameter does not depend on nanocrystal size, to within our resolution, for the larger particles ($a_{67}=7.90\pm 0.02$ Å, $a_{37}=7.91\pm 0.01$ Å, and $a_{20}=7.924$ Å²⁶), however, a comparison of the unit cell lengths of the large crystallites and the 6 nm crystallites indicates that there may be a slight particlesize dependence, with a unit cell length of both $a_6=7.84$ and 7.89 Å quoted in Ref. 27.

There is no simple explanation for the trend in the bulk modulus in terms of interatomic forces. In particular, our measurements are sensitive only to the strain within each nanocrystal, so cannot be due to a compressible intercrystalline region becoming more influential with decreasing crystal size. Nevertheless, in the spirit of the Debye model, increased compressibility is compatible with increased vibrational entropy (at a given temperature) for decreasing nanocrystal size. This, in turn, would lead to a decreasing melting temperature with decreasing size.

There has been a limited amount of work on the size dependence of the bulk modulus, and no consistent trend has been observed for different materials. From the reported work, some materials exhibit an enhancement of bulk modulus with decreasing particle size,^{13,14} while others show compressibility similar to their bulk counterparts. However, a few contrary examples are also reported: a decrease in bulk modulus with decreasing nanocrystal size may hold true for PbS and CdSe.^{32,33}

With hydrostatic compression the diffraction patterns evolve, becoming more complicated at pressures above 50.6 (56.3) GPa for 67 (37) nm γ alumina. The 400 peak becomes a doublet, and some of the low-intensity peaks are no longer visible (Fig. 1). By 55 (60) GPa, additional peaks not due to the γ phase of alumina are readily resolvable. The four new peaks have been indexed to a cubic phase which has not been previously identified. The new, high-pressure phase is retained upon decompression to 0 GPa.¹¹

The fact that the smaller nanocrystals transform at a higher pressure, although they are also more compressible than the larger nanocrystals, is notable in suggesting that the γ phase is indeed surface stabilized relative to both the α and the new (cubic) phase. That is, the strain energy at the transition is about 40% larger for the 37 nm than the 67 nm particles, implying much more stabilization of the smaller γ -Al₂O₃ nanocrystals relative to the high-pressure phase as long as the kinetics of transformation are not very different for the two sizes.

CONCLUSION

High-pressure quasihydrostatic x-ray diffraction experiments show that the compressibility of γ -alumina nanocrystals increases significantly with decreasing crystallite size between 20 and 67 nm. A phase of alumina has been synthesized by quasihydrostatic compression of nanophase γ alumina to pressures greater than 51 GPa (56 GPa) at room temperature for 67 (37) nm particles. This phase is cubic, but cannot be indexed to any of the known phases of alumina; it

represents a new structure of Al_2O_3 that is quenchable to 0 GPa. Synthesis of this new phase, by using nanocrystalline starting materials, illustrates a novel method for the creation of new crystal structures of common compounds.

ACKNOWLEDGMENTS

The authors wish to thank Dr. Jingzhu Hu for help at NSLS. This work was supported by the National Science Foundation and the Petroleum Research Foundation.

-
- ¹H. Gleiter, *Prog. Mater. Sci.* **33**, 223 (1989).
²A. S. Edelstein and R. C. Cammarata, *Nanomaterials: Synthesis, Properties and Applications* (Institute of Physics, Bristol, 1996).
³J. Schiotz, F. D. DiTolla, and K. W. Jacobsen, *Nature (London)* **391**, 561 (1998).
⁴T. van Buuren, L. N. Dinh, L. L. Chase, W. J. Siekhaus, and L. J. Terminello, *Phys. Rev. Lett.* **80**, 3803 (1998).
⁵A. N. Goldstein, C. M. Echer, and A. P. Alivisatos, *Science* **256**, 1425 (1992).
⁶C. C. Chen, A. B. Herhold, C. S. Johnson, and A. P. Alivisatos, *Science* **276**, 398 (1997).
⁷J. Z. Jiang, L. Gerward, D. Frost, R. Secco, J. Peyronneau, and J. S. Olsen, *J. Appl. Phys.* **86**, 6608 (1999).
⁸B. Chen, D. Penwell, M. B. Kruger, A. F. Yue, and B. Fultz, *J. Appl. Phys.* **89**, 4794 (2001).
⁹S. B. Qadri, E. F. Skelton, A. D. Dinsmore, J. Z. Hu, W. J. Kim, C. Nelson, and B. R. Ratna, *J. Appl. Phys.* **89**, 115 (2001).
¹⁰B. Chen, D. Penwell, and M. B. Kruger, *Solid State Commun.* **115**, 191 (2000).
¹¹C. Moffitt, B. Chen, D. M. Wieliczka, and M. B. Kruger, *Solid State Commun.* **116**, 631 (2000).
¹²J. Z. Jiang, J. S. Olsen, L. Gerward, D. Frost, and D. Rubie, *Europhys. Lett.* **50**, 48 (2000).
¹³Z. Wang, S. K. Saxena, V. Pischedda, H. P. Liermann, and C. S. Zha, *Phys. Rev. B* **64**, 012102 (2001).
¹⁴J. Z. Jiang, J. S. Olsen, L. Gerward, and S. Morup, *Europhys. Lett.* **44**, 620 (1998).
¹⁵R. E. Cohen, *Geophys. Res. Lett.* **14**, 37 (1987).
¹⁶K. T. Thomson, R. M. Wentzcovitch, and M. S. T. Bukowinski, *Science* **274**, 1880 (1996).
¹⁷N. Funamori and R. Jeanloz, *Science* **278**, 1109 (1997).
¹⁸S. Blonski and S. H. Garofalini, *Surf. Sci.* **295**, 263 (1993).
¹⁹J. M. McHale, A. Navrotsky, and A. J. Perrotta, *J. Phys. Chem.* **101**, 603 (1997).
²⁰J. M. McHale, A. Auroux, A. J. Perrotta, and A. Navrotsky, *Science* **277**, 788 (1997).
²¹J. Freim, J. McKittrick, J. Katz, and K. Sickafus, *Nanostruct. Mater.* **4**, 371 (1994).
²²R. S. Mishra, J. A. Schneider, J. F. Shackelford, and A. K. Mukherjee, *Nanostruct. Mater.* **5**, 525 (1995).
²³M. R. Gallas, B. Hockey, A. Pechenik, and G. J. Piermarini, *J. Am. Ceram. Soc.* **77**, 2107 (1994).
²⁴R. S. Mishra, C. E. Lesher, and A. K. Mukherjee, *J. Am. Ceram. Soc.* **79**, 2989 (1996).
²⁵T. M. H. Costa, M. R. Gallas, E. V. Benvenuti, and J. A. H. d. Jornada, *J. Phys. Chem. B* **103**, 4278 (1999).
²⁶M. R. Gallas and G. J. Piermarini, *J. Am. Ceram. Soc.* **77**, 2917 (1994).
²⁷J. Zhao, G. R. Hearne, M. Maaza, F. Laher-Lacour, M. J. Witcomb, T. L. Bihan, and M. Mezouar, *J. Appl. Phys.* **90**, 3280 (2001).
²⁸H. K. Mao, P. M. Bell, K. J. Dunn, R. M. Chrenko, and R. C. DeVries, *Rev. Sci. Instrum.* **50**, 1002 (1979).
²⁹D. L. Heinz and R. Jeanloz, *J. Appl. Phys.* **55**, 885 (1984).
³⁰F. Birch, *J. Geophys. Res.* **83**, 1257 (1978).
³¹I. Ohno, S. Yamamoto, and O. L. Anderson, *J. Phys. Chem. Solids* **47**, 1103 (1986).
³²S. B. Qadri, J. Yang, B. R. Ratna, E. F. Skelton, and J. Z. Hu, *J. Appl. Phys. Lett.* **69**, 2205 (1996).
³³S. H. Tolbert and A. P. Alivisatos, *Annu. Rev. Phys. Chem.* **46**, 595 (1995).